Immunolocalization of Sarcolemmal Dihydropyridine Receptor and Sarcoplasmic Reticular Triadin and Ryanodine Receptor in Rabbit Ventricle and Atrium

Stephanie Lewis Carl, Kelly Felix, Anthony H. Caswell,‡ Neil R. Brandt,‡ W. James Ball Jr.,* Pol L. Vaghy,* Gerhard Meissner,§ and Donald G. Ferguson

Department of Molecular and Cellular Physiology; *Department of Pharmacology and Cell Biophysics, University of Cincinnati, Cincinnati, Ohio 45267; ‡Department of Pharmacology, University of Miami, Miami, Florida 33101; and §Department of Biochemistry, University of North Carolina, Chapel Hill, North Carolina 27599

Abstract. The subcellular distribution of sarcolemmal dihydropyridine receptor (DHPR) and sarcoplasmic reticular triadin and Ca^{2+} release channel/ryanodine receptor (RyR) was determined in adult rabbit ventricle and atrium by double labeling immunofluorescence and laser scanning confocal microscopy. In ventricular muscle cells the immunostaining was observed primarily as transversely oriented punctate bands spaced at approximately 2-μm intervals along the whole length of the muscle fibers. Image analysis demonstrated a virtually complete overlap of the staining patterns of the three proteins, suggesting their close association at or near dyadic couplings that are formed where the sarcoplasmic reticulum (SR) is apposed to the surface membrane or its infoldings, the transverse (T-) tubules. In rabbit atrial cells, which lack an extensive T-tubular system, DHPR-specific staining was observed to form discrete spots along the sarcolemma but was absent from the interior of the fibers. In atrium, punctate triadin- and RyR-specific staining was also observed as spots at the cell periphery and image analysis indicated that the three proteins were co-localized at, or just below, the sarcolemma. In addition, in the atrial cells triadin- and RyR-specific staining was observed to form transverse bands in the interior cytoplasm at regularly spaced intervals of approximately 2 μm. Electron microscopy suggested that this cytoplasmic staining was occurring in regions where substantial amounts of extended junctional SR were present. These data indicate that the DHPR co-distributes with triadin and the RyR in rabbit ventricle and atrium, and furthermore suggest that some of the SR Ca^{2+} release channels in atrium may be activated in the absence of a close association with the DHPR.

IN striated muscle, depolarization of the sarcolemma and transverse (T-)[1] tubular network induces release of Ca^{2+} from internal stores in the sarcoplasmic reticulum (SR) by a process commonly referred to as excitation–contraction (EC) coupling. In skeletal muscle it is generally accepted that the electrical signal is transduced to a release of Ca^{2+} at specialized triad junctions formed between a central T-tubule flanked by two elements of closely apposed junctional SR (jSR). The junctional T-tubules contain DHPR which act as voltage sensors (36, 45, 56–58) and the junctional SR has

Address all correspondence to D. G. Ferguson at his current address, Department of Anatomy, Case Western Reserve University, 10900 Euclid Ave., Cleveland, OH 44106-4930. Tel.: (216) 368-1977. Fax: (216) 368-8669.

P. Vaghy's present address is Department of Medical Biochemistry, Ohio State University, Columbus, OH 43210.

1. *Abbreviations used in this paper:* DHP, dihydropyridine; DHPR, DHP receptor; jSR, junctional sarcoplasmic reticulum; RyR, ryanodine receptor; SR, sarcoplasmic reticulum; T-tubule, transverse tubule; TC, terminal cisternae.

rows of "feet" (23) that have been identified as ryanodine receptors (RyR), the SR Ca^{2+} release channels (35, 55, 61). The exact mechanism of skeletal muscle EC coupling is not yet completely understood; however, it is thought that the release of Ca^{2+} from the SR is a depolarization-induced mechanism without the necessity of Ca^{2+} flow (46). In contrast, excitation contraction coupling in cardiac muscle requires an influx of Ca^{2+} through L-type Ca^{2+} channels (the cardiac isoform of the DHP receptors), followed by Ca^{2+}-induced Ca^{2+} release from internal stores (12, 16, 17, 22, 39). Cardiac muscle cells do not have triads but there are dyadic couplings, formed between elements of sarcoplasmic reticulum and either the sarcolemma or the transverse tubules. Despite the apparent differences in the mechanisms of EC coupling, the dyadic junctions of cardiac muscle cells have long been considered to be the equivalents of the skeletal muscle triads. Indeed, the cardiac junctional sarcoplasmic reticulum (jSR) contains ryanodine-sensitive Ca^{2+} release channels (1, 25, 44) and cardiac muscle sarcolemma

and T-tubules are thought to contain dihydropyridine (DHP)-sensitive Ca^{2+} channels (2, 7, 8). Nonetheless, the characterization of the dyads is still based primarily on their ultrastructural appearance in thin sections prepared for transmission electron microscopy. In mammalian cardiac myocytes, dyads are observed as peripheral couplings formed between the sarcolemma and flattened elements of jSR which clearly have "feet" on their surface, or as internal couplings which are formed between jSR and tubules of the T-network (20, 27, 28, 50, 51). Immunolocalization of the proteins of the dyadic junctional region has been limited to the jSR luminal Ca^{2+} binding protein, calsequestrin (29, 30) and recent reports describing the distribution of the RyR in ventricle and Purkinje conducting fibers (31) and avian cardiac muscle (32). The most detailed evidence concerning the disposition of putative DHP receptors is still the relatively indirect freeze fracture information from skeletal muscle (4, 24) in which tetradic arrays of particles have been proposed to represent the DHP receptor (DHPR). Although a recent study compared the distribution of the cardiac DHPR to that of the sarcolemmal Ca^{2+}-ATPase and Na^+/Ca^{2+} exchanger (26), as yet there is no immunolocalization data comparing the disposition of the cardiac DHPR to that of the other dyadic proteins. Thus, despite preliminary, indirect evidence from Ca^{2+} influx and release studies (48), or predictions based on theoretical considerations (52), the important question as to whether the DHP receptors are clustered and associated with adjacent elements of jSR in the dyads, or are randomly dispersed throughout sarcolemma remains unanswered.

Recently, a 95-kD protein, triadin, has been purified from junctional SR fractions (11), localized to the triad region in adult (33, 34) and developing rat skeletal muscle (our own unpublished observations) and cultured skeletal muscle cells (19). Triadin has been suggested as a candidate for the protein which maintains a linkage between the DHPR and the ryanodine receptor (RyR) (9, 11). We have previously shown that triadin may be a component of the cardiac dyads in rat ventricular cells (10) but no comprehensive examination as to its relationship with other dyad proteins has been performed.

In this study, we have immunolocalized triadin, the RyR, and the DHPR complex in atrial and ventricular tissue of adult rabbits using double labeling immunofluorescence and laser scanning confocal microscopy. We have also used transmission electron microscopy to examine the ultrastructure of ventricular and atrial cells to complement the immunofluorescence data.

Materials and Methods

Antibody Production, Purification, and Characterization

The triadin monoclonal antibody, AE 8.91 was raised as previously described (10).

Mouse monoclonal antibodies were raised against DHPR complexes that were purified from rabbit skeletal muscle (60), using standard techniques as previously described (3). Western blots were used to demonstrate that the monoclonal antibodies used for this study were specific for the $\alpha2$ subunit of the skeletal muscle DHPR (data not shown). For immunofluorescence, the ascites fluid of the most effective antibody, 6B5, was further purified using protein A chromatography and a centricon 30 system was used to concentrate the antibodies to 1 mg/ml as determined by a Bradford assay.

Monoclonal antibody C3-33, against the canine cardiac ryanodine receptor, was raised in BALB/c mice immunized by serial injection of canine cardiac SR vesicles and the purified ryanodine receptor as previously described (47). The antibody was purified by protein A chromatography and the specificity was determined by immunoblot analysis (47).

Monoclonal antibody specific for sarcomeric myosin (MF20) was obtained as ascites fluid from the Developmental Studies Hybridoma Bank (Iowa City, IA).

In addition, specificity of the primary antibodies was also determined using immunoblots prepared from crude membrane fractions of adult rabbit atrium and ventricle. Briefly, tissue was cut into small pieces and homogenized in a Sorvall Omnimixer for 30 seconds in 5 volumes of 10 mM histidine/10% sucrose (pH 7.2). Cellular debris was pelleted at 12,000 g for 15 min and the crude microsomal pellet was obtained from the resultant supernatant by centrifugation 180,000 g for 30 min. For gel electrophoresis, 0.8 mg of the pellet was extracted in 4 ml of SDS reducing buffer. The extracts were subjected to electrophoresis on 6% polyacrylamide gels in the presence of SDS, and proteins were electrophoretically transferred to a nitrocellulose membrane. To prepare Western blots, the membranes were blocked for 5 min with 0.05% Tween in TBS at pH 7.5, incubated for 60 min with the primary antibodies, washed with Tween/TBS and incubated for 60 min with an appropriate alkaline phosphatase-conjugated secondary antibody. The alkaline phosphatase activity was detected on the membranes using nitro blue tetrazolium and 5-bromo-4-chloro-3-indolyl-phosphate as substrate according to ProtoBlot instructions (Promega Biotech, Madison, WI).

Tissue Collection and Cryosectioning

Young adult rabbits were anesthetized with sodium pentobarbital and perfused through the left ventricle with relaxing solution (0.1 M KCl, 5 mM EGTA, 5 mM $MgCl_2$, 5 mM Na pyrophosphate, 0.25 mM dithiothreitol, and 10 mM histidine at pH 6.8; for experiments in which myosin was to be localized Na pyrophosphate was omitted). Hearts were then excised and placed in ice cold relaxing solution. The atria and left ventricular papillary muscles were dissected out, pinned at approximately resting sarcomere length in relaxing solution, trimmed to 5 × 1-mm strips, mounted on cork specimen holders using gum tragacanth, and flash frozen in liquid nitrogen-cooled isopentane. Frozen sections, 5 μm in thickness, were obtained using a Microm cryostat (Carl Zeiss, Inc., Batavia, IL), collected on gelatin-coated glass slides or Superfrost/Plus glass slides (Fisher Scientific, Pittsburgh, PA), and immunostained immediately.

Immunofluorescence Labeling

The strategy that we used to examine the distribution of the putative dyadic proteins was to sequentially co-localize pairs of the three antigens. Thus, the distributions of both triadin and the DHPR complex were compared to that of the RyR in indirect immunofluorescence double labeling experiments.

Prior to staining, sections were fixed to the slides using freshly prepared 4% paraformaldehyde for 15 min and washed (three changes of 5-min each) in PBS at pH 7.2. Double labeling experiments were performed in adult ventricle with the mouse triadin monoclonal antibody (AE 8.91) and the cardiac RyR monoclonal antibody (C3-33) to compare the distribution of these dyadic proteins. Since both of the primary antibodies are mouse monoclonals it was necessary to use a procedure that eliminates cross reactivity of the primary and secondary antibodies. Complete details of this protocol have been previously described (37). Briefly, sections were incubated in PBS containing 1% BSA to block nonspecific binding sites, followed by a 60-min incubation in AE 8.91, subjected to three PBS/BSA washes of 10 min each followed by a 60-min incubation in goat anti-mouse IgG (GaM) secondary antibodies conjugated to fluorescein (FITC). Excess secondary antibody was washed off using three 10-min changes of PBS/BSA. Sections were then incubated for 60 min in PBS/BSA containing a non-binding mouse monoclonal IgG antibody (anti-human IgE clone No. GE-1; Sigma Immunochemicals, St. Louis, MO) to block the free arms of the bivalent GaM-TRITC secondary antibody. This was followed by a 60-min treatment with GaM F(ab) fragments (Jackson ImmunoResearch Laboratories, West Grove, PA) to block all remaining cross-reactive sites. The sections were then immunostained using C3-33 mouse monoclonal antibodies which were detected with GaM conjugated to rhodamine (TRITC). Coverslips were mounted using a 70% glycerol/PBS mixture containing 4% 1,4-diazabicyclo[2,2,2]octane (DABCO). In parallel experiments, other sections were stained using mouse monoclonal antibodies raised against the $\alpha2$ sub-

unit of the DHPR (6B5) and the cardiac RyR (C3-33). In experiments to immunolocalize dyadic proteins in sections of adult rabbit atrium, AE8.91 (triadin) and 6B5 (DHPR) were again detected using GaM-FITC and C3-33 (RyR) was detected using GaM-TRITC.

In control experiments, sections were stained with 6B5 or AE8.91 using the above protocol but the incubation with C3-33 was omitted. This was to ensure that none of the observed staining was due to cross reactivity of the secondary antibodies. Double staining control experiments in which the order of the secondary antibodies was reversed and single staining control experiments were also performed.

Sections were examined using an inverted Nikon Diaphot fluorescence microscope. Laser scanning confocal images were collected, digitized and analyzed using CoMOS software (Bio-Rad Laboratories, Cambridge, MA). For comparison of staining patterns, digitized images from the FITC and TRITC channels were acquired from the same area of the section and were merged (superimposed) to determine how much overlap was present in the staining patterns arising from the different antibodies. Indirect immunofluorescence is not a rigorously quantitative technique, especially when comparing signals from two distinct primary antibodies. For example, differences in binding affinities of the primary antibodies can greatly influence the amount of staining, irrespective of the absolute amounts of the antigens being localized. Thus, in order to obtain optimum merged images, the signals on each channel had to be balanced prior to merging. In this procedure, the brightest points in the signals on each channel were normalized by adjusting the sensitivity and the gain of the laser. Then each pixel on both channels was assigned a gray level value (from 0–255) based on the fluorescence intensity and the relative intensity on each channel was compared. The C3-33 ryanodine receptor antibody was observed to give the strongest signal and the gain (sensitivity) on that channel was set to ∿60% in comparison to the channel containing the 6B5 DHPR antibody signal and to ∿75% of that for the channel containing the AE 8.91 triadin antibody signal. The merged images were printed using a Sony UP5000 video color printer.

Electron Microscopy

Young adult rabbits were anesthetized with sodium pentobarbital and the heart was removed and attached to a Langendorff perfusion apparatus. The heart was equilibrated for 5 min with oxygenated Krebs solution and then perfused with fixative (2.5% glutaraldehyde in 0.1 M Na cacodylate). Thin strips of atrial and ventricular tissue were fixed in glutaraldehyde for 60 additional min, washed in 0.1 M cacodylate, postfixed in 1% osmium tetroxide, washed in cacodylate, dehydrated in a graded series of ethanol and embedded in Epon epoxy resin. Thin sections, obtained using a Reichert Ultracut S, were stained in uranyl acetate and lead citrate and examined in a Zeiss EM10 transmission electron microscope.

Results

Immunoblots

The C3-33 cardiac ryanodine receptor antibody detected a single, high molecular mass band in transblots of crude membrane extracts from both atrial (Fig. 1 A) and ventricular (Fig. 1 B) tissue of adult rabbits. The 6B5 DHPR α2 subunit antibody detected a single band with a molecular mass of approximately 160 kD in transblots of crude membrane extracts from both atrial (Fig. 1 C) and ventricular (Fig.1 D) tissue of adult rabbits. The AE 8.91 triadin antibody detected a band of approximately 95 kD in transblots of crude membrane extracts from both atrial (Fig. 1 E) and ventricular (Fig. 1 F) tissue of adult rabbits. The relatively broad band obtained with the AE 8.91 is typical of a glycoprotein such as triadin. These data indicate that the primary antibodies all bind specifically to antigens of the predicted relative molecular weight and are appropriate for use in the immunofluorescence studies carried out in this study.

Immunofluorescence

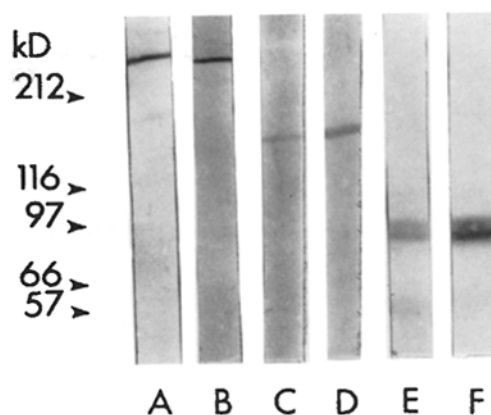To compare the distribution of triadin and the RyR, longitu-

*Figure 1.* Western blots of adult rabbit atrial and ventricular muscle microsomes. (*A, C,* and *E*) Atrium; (*B, D,* and *F*) ventricle. (*A* and *B*) C3-33 (RyR); (*C* and *D*) 6B5 (DHP receptor α2 subunit); (*E* and *F*) AE8.91 (triadin). These transblots were prepared following the procedures outlined in the materials and methods section. The blots contain single bands for each antibody at apparent molecular weights consistent with that expected for the respective junctional proteins.

dinal sections of rabbit ventricular muscle were incubated with the AE 8.91 triadin antibody and the C3-33 cardiac RyR antibody. The binding sites of these antibodies were detected using GaM-FITC (Fig. 2 *A*) and GaM-TRITC (Fig. 2 *B*), respectively. In these sections, the predominant staining pattern is observed to be regularly-spaced transverse bands with a periodicity of ∿2 μm. This spacing is consistent with the notion that the RyR (and triadin) are contained in dyadic junctions along the length of the T-tubules situated at the Z lines. However, the high level of staining suggests that the dyads may be more extensive than commonly depicted in diagrams of cardiac muscle ultrastructure (5, 49). Punctate staining was also observed to be associated with discrete regions of the sarcolemma (Fig. 2 *C, arrows*). This was a minor feature compared to the striated bands in the cytoplasm and likely represents staining associated with peripheral couplings.

To compare the amount of overlap in the staining patterns obtained using the triadin and RyR antibodies (and thus determine the degree to which the two proteins are co-distributed), the image pairs were analyzed using CoMOS software and merged images were produced as described in Materials and Methods. In the merged images, areas in which the intensity on the FITC channel was high but intensity on the TRITC channel was low, appear green. Conversely, areas in which the fluorescence signal was high on the TRITC channel but low on the FITC channel, appear red. Areas in which the intensity was high on both channels would appear yellow in the merged images and would indicate that the two antigens were co-distributed, at least at the limits of resolution of the laser scanning confocal microscope (∿0.1 μm).

In the merged images obtained from Fig. 2 (*A* and *B*) the preponderance of the color arising from specific staining is yellow (Fig. 2 *C*), suggesting that there is essentially complete overlap of triadin and RyR staining, and thus, triadin

676
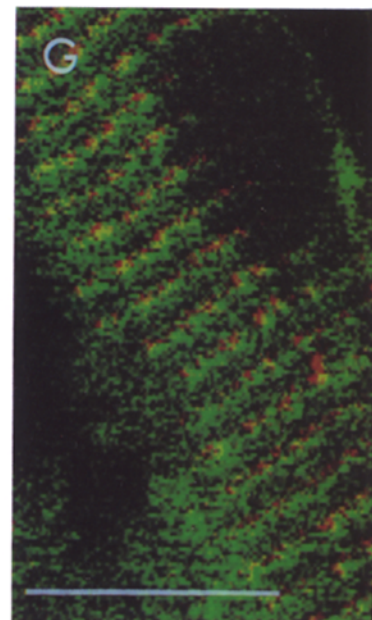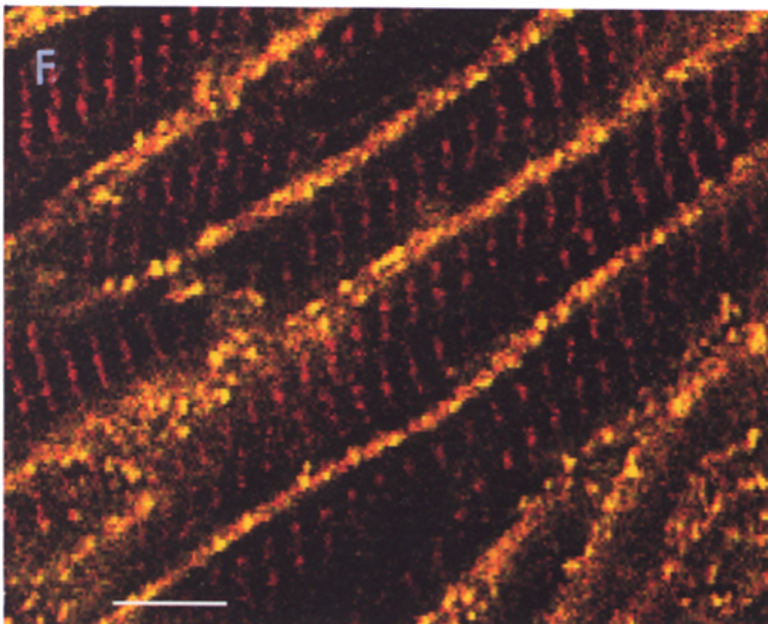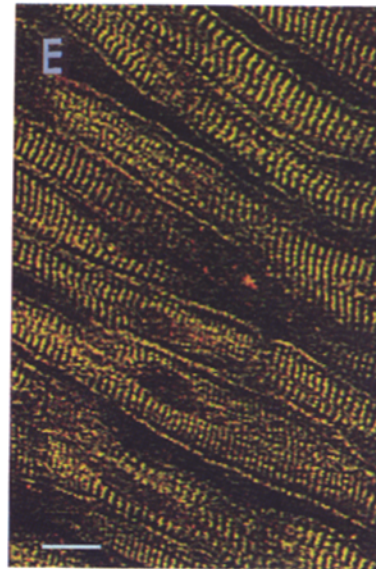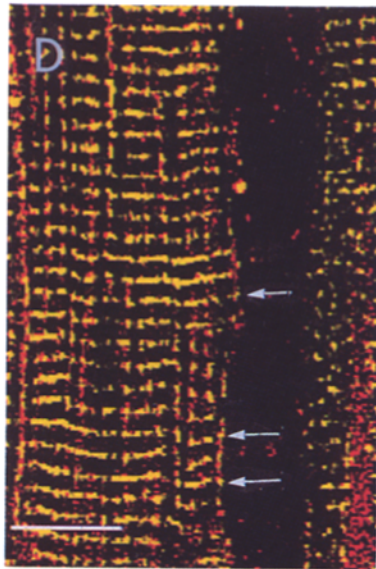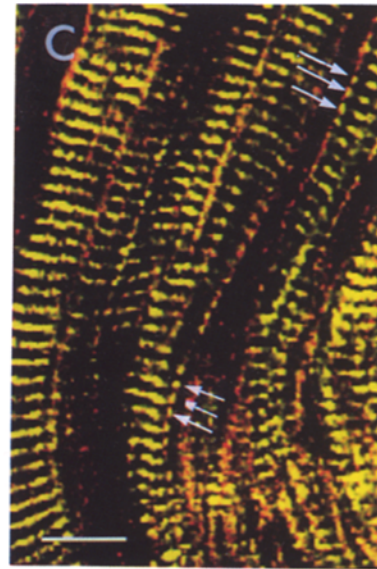
and the RyR are likely dyadic proteins in ventricular cardiac muscle.

There were a few relatively thick longitudinal streaks on the TRITC channel (Fig. 2 B) which appeared to be located primarily at the edges of the cells. This signal is also visible as longitudinal reddish streaks in the merged image (Fig. 2 C). Since this staining is not very distinct or well localized, we believe that it represents non-specific background staining. Several control experiments support this interpretation. The streaks are not present in single staining experiments with either secondary antibody; and when the secondary antibodies are reversed so that the RyR-specific primary antibody is detected with an FITC-conjugated secondary antibody and the triadin-specific primary antibody is detected with a TRITC-conjugated antibody the slight excess staining is still observed on the TRITC channel (not shown).

To compare the distribution of the cardiac DHPR with that of the RyR, longitudinal sections of rabbit ventricular cardiac muscle were stained with the 6B5 skeletal muscle DHPR α2 subunit antibody and the C3-33 cardiac RyR antibody. In merged (superimposed) images produced as described above, the staining again forms regularly-spaced transverse yellow bands ∼2-μm apart (Fig. 2 D). This predominantly yellow color indicates that the RyR and the DHPR complexes are co-distributed. The spacing suggests that they may be contained in dyadic junctions situated at the Z lines (see also Fig. 2 G). There are also a few discrete spots associated with the sarcolemma (Fig. 2 D, arrows) which likely represent staining of peripheral couplings.

Non-specific background staining was again present as a minor feature on the TRITC channel and gives rise to longitudinal reddish streaks in the merged image (Fig. 2 D). Again, these streaks were not observed in single staining experiments; and when the secondary antibodies were reversed so that RyR was detected with FITC and DHPR with TRITC, the excess staining was still observed on the TRITC channel (not shown).

A unique feature of the myocardium of some mammals is that there are distinct regional differences in the ultrastructure of the T-system. Rabbit ventricular cells have a well developed T-system and many internal dyadic couplings are observed along the length of the T-network (5, 20, 21, 49, 51). In contrast, the atrial cells have little or no T-system, and dyads are restricted to the surface (peripheral couplings), where they are relatively more numerous than in ventricular cells (6, 51). However, the cytoplasm of these atrial cells has been observed to contain a form of SR that bears feet structures on its surface but does not form dyadic junctions. This type of SR has come to be known as extended junctional SR (27) and is often observed as small spherical outpocketings called corbular SR (14). To examine the distribution of the putative dyadic proteins in cardiac muscle cells that have a poorly developed T-system, sections of adult rabbit atrial muscle were stained with the AE 8.91 triadin antibody and the C3-33 cardiac RyR antibody. In atrium, the RyR was detected with TRITC-conjugated secondary antibodies; triadin and the DHPR complex were detected with FITC-conjugated secondary antibodies. In merged images from these samples the predominant color was again yellow, indicating co-distribution of triadin and the RyR (Fig. 2 E). However, in contrast to the ventricular cells, there was also a considerable amount of staining in the region of the sarcolemma (Fig. 2, compare C and E). The punctate line of yellow suggests that there are substantial numbers of subsarcolemmal elements of junctional SR in these atrial cells. This might have been predicted based on the previously reported abundance of peripheral couplings in atrial cells (6, 21, 28, 51). On the other hand, in the cytoplasm we also observed regularly-spaced transverse yellow bands ∼2-μm apart (Fig. 2 E). This was somewhat unexpected in these cells that are thought to be essentially devoid of T-tubules.

To examine this further, sections of adult rabbit atrial cardiac muscle were stained with the 6B5 DHPR α2 subunit antibody and the C3-33 cardiac RyR antibody. In merged im-

Figure 2. Indirect immunofluorescence localization of triadin, DHP receptor complex and ryanodine receptor in adult rabbit heart tissue. These image pairs were produced using a laser scanning confocal microscope to examine sections prepared by the double staining protocol outlined in the materials and methods section. The triadin- and the DHPR-specific primary antibodies were detected with secondary antibodies conjugated to FITC and the RyR-specific antibody was detected with secondary antibodies conjugated to TRITC. (A and B) Immunolocalization of RyR (A) and triadin (B) in ventricle. The predominant staining pattern is observed to be striations spaced at regular intervals of ∼2 μm. This is consistent with the known distribution of the T-system at the level of the Z lines in ventricular myocardial cells. (C) Merged image produced by superimposing A and B. Essentially all of cytoplasmic staining and the staining in the sarcolemmal region which appears to arise from antigen-specific labeling gives rise to yellow. This indicates that the staining patterns overlap and that the RyR and triadin are co-distributed. There are also a few small discrete regions close to the sarcolemma that are stained (arrows). These likely represent subsarcolemmal peripheral couplings. (D) Immunolocalization of RyR and DHPR in ventricle. Merged image generated from a double staining experiment to co-localize the DHP receptor α2 subunit and ryanodine receptor in the same section. Again, essentially all of cytoplasmic staining (regularly spaced transverse bands) and the punctate staining at the sarcolemma which arises from antigen-specific staining (small spots at arrows) produces yellow. This suggests that the DHPR is abundant in the tubules of the T-network and discrete regions of the sarcolemma and is codistributed with the RyR in adult rabbit ventricular cells. (E) Immunolocalization of the RyR and triadin in atrium. The predominant color in this merged image is yellow indicating that triadin and the RyR are also co-distributed in rabbit atrial cells. The staining associated with the sarcolemmal region is much heavier than was observed with these antibodies in ventricular cells (Fig. 2, A–C). This staining has the appearance of a line of spots that forms a boundary for each cell. Many of the spots are observed to line up with the regularly spaced transverse bands in the cytoplasm. (F) Immunolocalization of RyR and DHPR in atrium. In the atrium, the DHPR α2 subunit antibodies were detected using secondary antibodies conjugated to FITC and the RyR antibodies were detected using GaM-TRITC. The merged images contain regularly spaced transverse red bands clearly confirming the existence of cytoplasmic arrays of RyR. The sarcolemmal region is again demarcated by lines of discrete yellow spots. This suggests that the DHPR must be clustered in the sarcolemma in close association with elements of subsarcolemmal junctional SR. (G) Co-localization of RyR and myosin in adult rabbit atrium. In this longitudinal section, RyR-specific staining is observed as red transverse lines and myosin-specific staining is observed as broad green bands. The sarcomeric spacing in this sample was ∼2 μm, suggesting that the cells were somewhat contracted. At this sarcomere length the red and green signals are somewhat close to each other and a slight yellow-green color is present at the border of the red and green signals. Bars: (A–E, and G) 10 μm; (F) 5 μm.

ages from this experiment, in which the C3-33 was detected with rhodamine, a substantial amount of RyR-specific staining is observed as regularly spaced, transverse red bands in the cytoplasm of the atrial cells (Fig. 2 F). The red color of the striated bands indicates that there is no co-distribution of RyR staining with DHPR staining (which would give rise to yellow). This suggests that if these atrial cells do contain a T-network that the T-tubules do not contain DHPR, or more likely that rabbit atrial cells lack a T-system. Furthermore, it confirms that these cells have extensive, well-organized arrays of extended jSR in the cytoplasm. Apparently an interaction between DHPR and RyR is not essential for the organization of the extended jSR in these cells.

On the other hand, the staining in the sarcolemmal regions, is observed as discrete yellow spots (Fig. 2 F). This indicates that not only are the DHPR complexes restricted to the sarcolemma, they are clustered and are closely associated with RyR that are presumably contained on subsarcolemmal elements of jSR. In addition, since the yellow spots often appear to be in register with the striated bands

in the cytoplasm (Fig. 2 F), the peripheral couplings may not be randomly dispersed but may be positioned primarily at the Z-lines.

A characteristic of the optical system used for these studies is that when "tuned" for double staining experiments, the image on the TRITC channel is not as sharp as that on the FITC channel. This appears to give rise to red halos around many of the yellow spots or a reddish haze between adjacent cells in the merged images in Fig. 2 F. This was not observed in single staining experiments and when the order of application of the secondary antibodies is reversed so that the RyR is detected with FITC and the DHPR is detected with TRITC, the excess staining remains on the TRITC channel (not shown).

In the ventricle, the interpretation that the well-organized cytoplasmic staining arises from dyadic junctions located at the Z-lines is consistent with the extensive ultrastructural literature that has demonstrated the existence of a well-developed T-network at each Z-line along which dyadic couplings with the SR are abundant (5, 14, 20, 21, 51). To
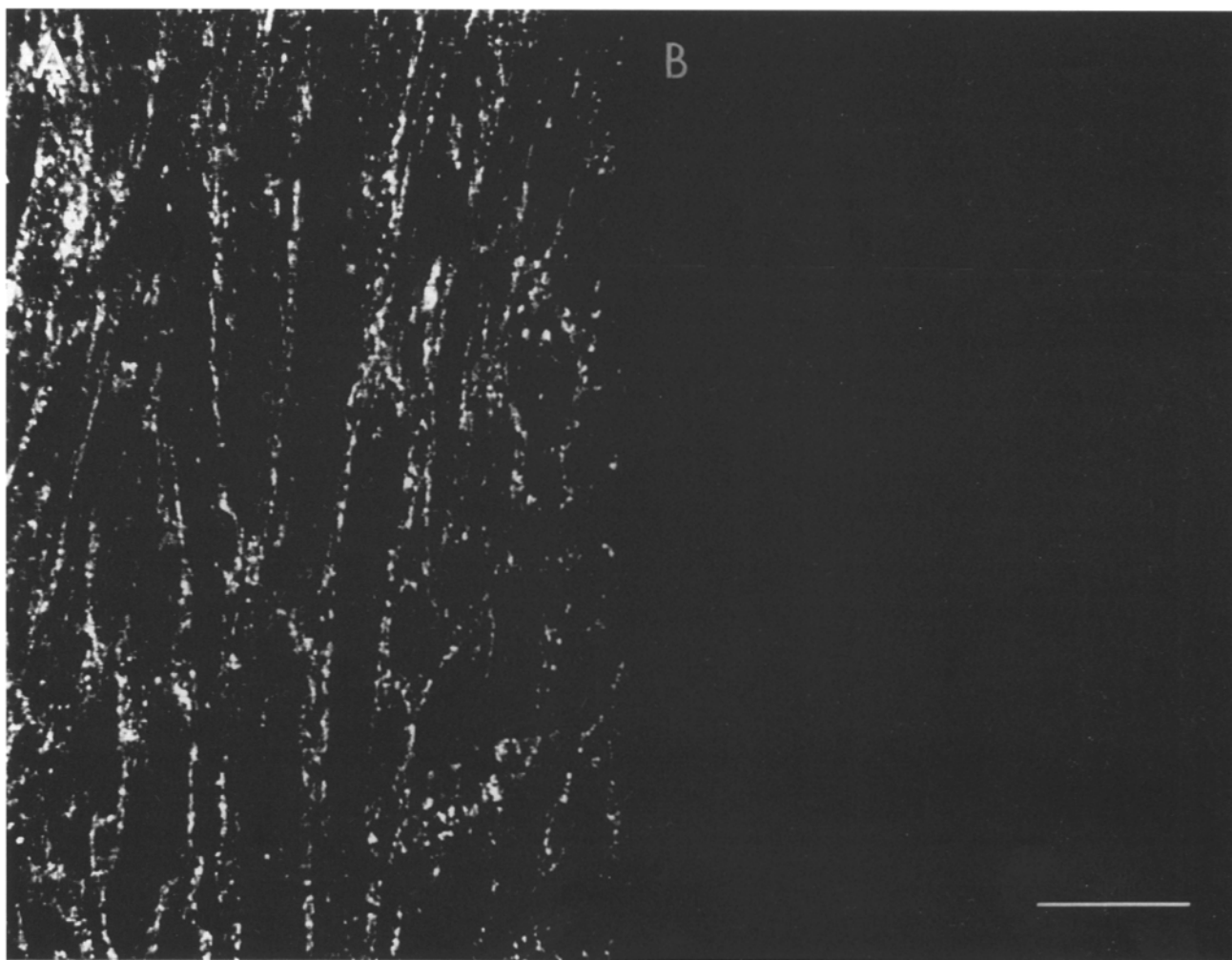

Figure 3. Adult rabbit atrium stained with the 6B5 DHP receptor $\alpha 2$ subunit antibody. In this control procedure, the section was prepared using the double staining procedure outlined in Materials and Methods except that the second primary antibody (C3-33, anti–RyR) was omitted. The absence of signal on the second (TRITC) channel indicates that blocking was complete. Thus, the overlap of staining patterns observed in the merged images in Fig. 2 is not due to cross reactivity of the secondary antibodies.

examine the positioning of the extended jSR in atrial cells, myosin and the RyR were co-localized in longitudinal sections of adult rabbit atrium. In these experiments there was essentially no overlap of the myosin-specific and the RyR-specific staining (Fig. 2 G). Based on the universally accepted structure of the sarcomere of striated muscle, myosin-containing thick filaments compose the A band and the Z-line is in the middle of each I band. The lack of overlap of the RyR- and myosin-specific staining is strong, indirect evidence that the RyR-specific staining is located at the Z-lines.

Control experiments were performed to demonstrate that there was no cross-reactivity between the two sets of primary and secondary antibodies in the double staining experiments. In these experiments, frozen sections of both atrium and ventricle were incubated with either the 6B5 DHPR α2 subunit antibody or with the AE 8.91 triadin antibody. The sections were subsequently stained according to the protocol described in the materials and methods except that the second primary antibody (C3-33) was omitted. All these control experiments were performed at the same time as the double staining experiments. Thus, the laser settings for both channels were optimized using the appropriate double stained section and then the control section was immediately placed on the microscope. Therefore, the gain and sensitivity for the control sections was identical to that for the double staining experiments depicted in Fig. 2. In all the control experiments no staining was detectable on the second channel. Fig. 3 is an example of one of these control experiments using the 6B5 DHPR α2 subunit antibody in atrial tissue.

Electron Microscopy

The ultrastructure of the dyads in ventricular and atrial tissue was examined to complement the immunofluorescence data.

In the ventricular cells, it is possible to find examples of peripheral couplings (Fig. 4 A) but they are not abundant. Internal dyads along the T-tubules represent the predominant form of coupling in ventricular cells (Fig. 4, B and C). Dyads are formed between relatively large diameter T-tubules and flattened elements of jSR, identified on the basis of the feet located on the surface. The dyads are quite abundant, most of the T-tubules in any given field have dyadic couplings associated with them (Fig. 4 C). In atrial cells, dyads are observed primarily as peripheral couplings which are larger and more numerous than the subsarcolemmal dyads observed in ventricular cells (Fig. 5 A). The level of staining in the immunofluorescence images indicated that there was an abundance of extended jSR in the cytoplasm and the spacing and localization with respect to myosin suggests that the stained elements are at the Z-lines. Since the transverse bands that we observed in the immunofluorescence experiments were extensive, one might expect to observe longer cisternal elements in the electron micrographs. However, we were not able to detect any cisternal elements of extended jSR. Instead, at or near the Z-lines, we observed numerous small round membrane profiles with feet on their cytoplasmic surface (Fig. 5, B and C). This suggests that the immunofluorescence data may result from regularly disposed elements of corbular SR (Fig. 5 C).

Discussion

We have previously demonstrated that a skeletal muscle triadin-specific monoclonal antibody (GE 4.90) binds to a 95-kD protein that co-distributes with junctional markers when rat cardiac microsomes are centrifuged on isopycnic gradients (10). Furthermore, in indirect immunofluores-
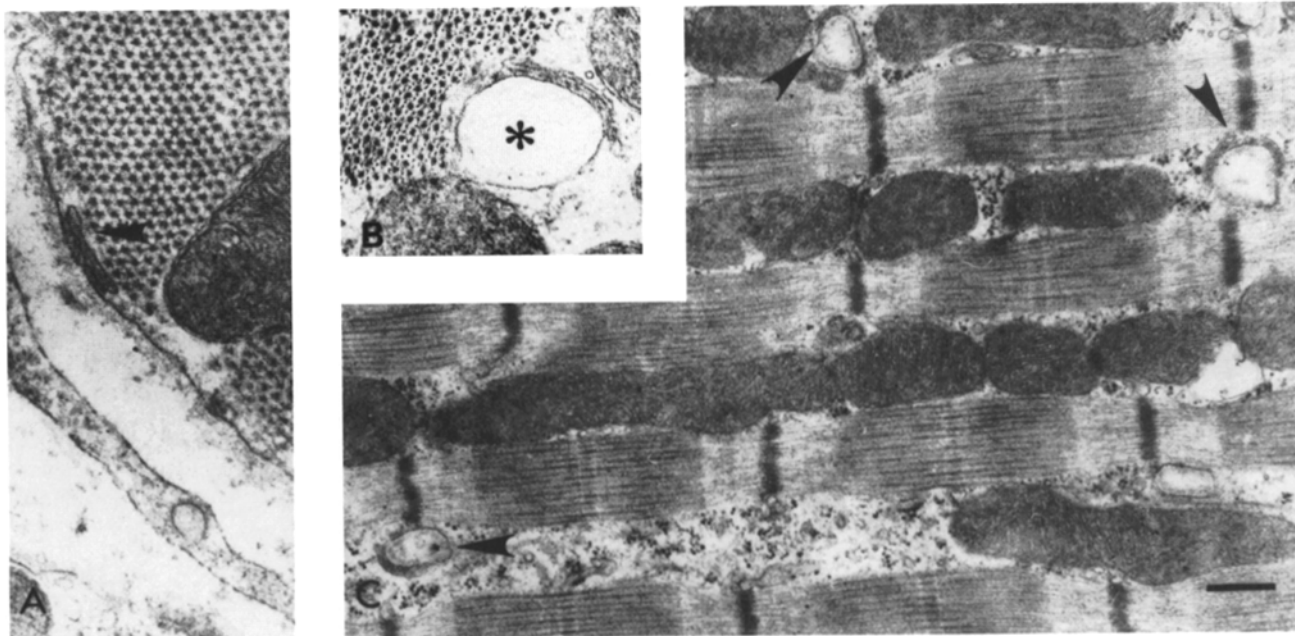

Figure 4. Rabbit ventricle ultrastructure. (A) A peripheral coupling (*arrowhead*) is observed as an element of subsarcolemmal SR with feet on the junctional surface in close apposition to the adjacent sarcolemma. (B) An internal coupling (*) is formed between a dilated T-tubule and an element of jSR. (C) Internal couplings (*arrowheads*) are observed at many Z-lines in this longitudinal section. Most of the elements of the T-network have jSR associated with them, confirming the immunofluorescence staining patterns which indicated that the dyads were extensive. Bars: (A and B) 185 nm; (C) 370 nm.

cence experiments using GE 4.90, staining was observed as transverse bands with a periodicity of ~2 μm in detergent-treated longitudinal sections of adult rat ventricle (10). The mRNA for triadin have also previously been detected in cardiac muscle using Northern blot analysis (43). In the present study, we have used an alternative skeletal muscle triadin-specific antibody, AE 8.91. We have determined that the epitope for AE 8.91 appeared to be more accessible in that detergent treatment was not required to obtain staining in indirect immunofluorescence experiments. Thus, although both antibodies give identical staining patterns in skeletal and cardiac muscle (unpublished observations), we have observed that AE 8.91 was more effective for the double labeling studies because the morphological preservation of the tissue was better than that obtained with GE 4.90. In other respects, the properties of AE 8.91 as an immunoprobe were indistinguishable from those of GE 4.90: it binds specifically to a 95-kD protein in immunoblots of rabbit atrial and ventricular cardiac muscle, and appears to selectively stain the junctional SR of these cells. The observation that triadin is a component of the cardiac dyads is in contrast to a previous study that did not detect either the triadin message or protein in cardiac muscle tissue (34). The most likely explanation for this discrepancy is that there are skeletal and cardiac muscle isoforms of triadin. Thus, the probes used in the previous study (34) may detect an epitope in the skeletal muscle isoform of triadin that is not present in the cardiac isoform, whereas both GE 4.90 and AE 8.91 bind to epitopes that are conserved in the cardiac and skeletal muscle isoforms.

In these studies, we have observed that triadin is co-distributed with the RyR and the DHPR in ventricular myocytes and in the peripheral couplings of atrial cells but is associated preferentially with the RyR in the extended jSR of atrial cells. This latter finding is consistent with the distribution observed in cultured dysgenic skeletal muscle cells that contain no α1 subunit of the DHPR (19). These cells were observed to have disorganized T-networks and few triad junctions but triadin and the RyR were still co-distributed, largely in the absence of an interaction with the DHPR (19). Thus, while triadin is clearly a jSR protein, its role in cardiac muscle needs to be clarified. Since a considerable proportion of the triadin in atrial cells is associated with the RyR in the absence of the DHPR, it appears unlikely that in cardiac cells its only function is to link these two proteins.

The 6B5 antibody that we used to immunolocalize the cardiac DHPR complex was raised against the α2 subunit of the skeletal muscle DHPR. However, only a single gene has been identified for the α2 subunit of the DHPR (15) and antibodies raised against the α2 subunit of the skeletal muscle DHPR by several different laboratories have previously been used to detect the α2 subunit of the cardiac DHPR on Western blots (41) and to immunoprecipitate the whole DHPR complex from cardiac membranes (54, 59). Therefore, we believe that the 6B5 antibody, which binds specifically to the cardiac α2 subunit of the DHPR, is an effective immunoprobe for the cardiac DHPR complex.

In the present studies, we have used the 6B5 antibody and the C3-33 cardiac RyR-specific antibody to co-localize these proteins in both atrial and ventricular cells of adult rabbit heart. We have found that in adult rabbit ventricular cells, immunostaining attributable to co-localization of the RyR
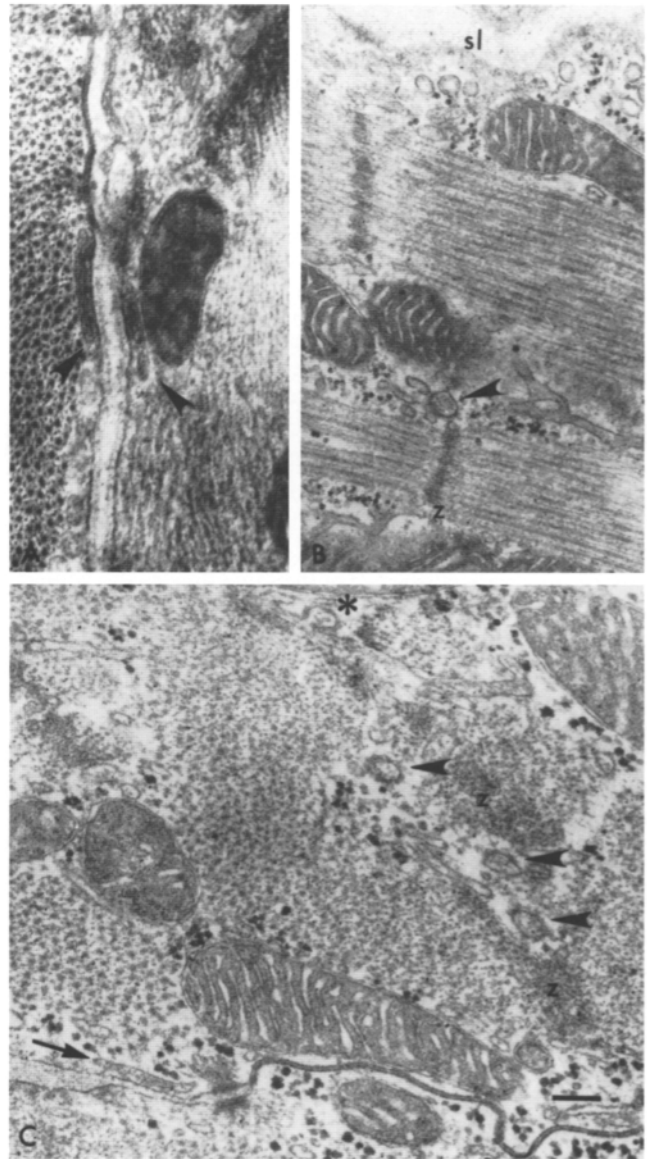

Figure 5. Rabbit atrium ultrastructure. (*A*) This electron micrograph is a cross section of two atrial muscle cells. Peripheral couplings (*arrowheads*) are seen in each cell. (*B*) A longitudinal section containing profiles of non junctional SR between the myofibrils. An element of jSR (*arrowhead*) is observed at the level of the Z line (z) of one of the sarcomeres. (*C*) An oblique cross section in which the extended jSR is observed to form a series of small, apparently spherical structures (*arrowheads*). These structures are predominantly located at the level of the Z line (z) which in this view appears as a darker amorphous structure amongst the small discrete cross sections of the contractile filaments. One of these jSR structures appears to form a small outpocketing from nonjunctional SR (*). This suggests that the cytoplasmic staining observed in the immunofluorescence images may be arising from elements of corbular SR that are located at the Z lines. A peripheral coupling (*arrow*) is also observed at the lower left of the micrograph. Bars: (*A*) 122 nm; (*B*) 172 nm; (*C*) 138 nm.

and the DHPR forms transverse bands at regular 2-μm intervals and a few small spots in the sarcolemmal region. Within each transverse band, the staining is observed as discrete spots, suggesting that the proteins are localized rather than

being uniformly distributed. In atrial cells, the staining attributable to co-distribution of the RyR and the DHPR is restricted to the sarcolemmal region where it is observed as discrete, spots. Our electron microscopic studies indicate that in these areas, feet (RyR) are present only in the dyads. A previous study has demonstrated that the C3-33 antibody is an effective immunoprobe for the cardiac RyR/SR Ca^{2+} release channel that is equivalent the foot structure of jSR in EM images (32). Therefore, our immunofluorescence localization and complementary ultrastructural observations strongly suggest that the DHPR and the RyR are localized to internal and to a lesser extent to peripheral dyadic couplings in ventricle and to peripheral couplings in atrium. These findings constitute the first direct evidence that the cardiac DHP receptors are clustered and associated with adjacent elements of jSR. Studies in avian cardiac muscle provide immunolocalization data consistent with our findings and provide additional freeze fracture information concerning the disposition of putative DHPR in the sarcolemma (see refernce 53 for details).

This apparently preferential association of the cardiac DHPR with the RyR (and triadin) has important implications. The proposed cardiac excitation-contraction coupling signal transduction mechanism, an influx of Ca^{2+} followed by Ca^{2+}-induced Ca^{2+} release, removes the requirement for a direct physical interaction between the RyR and the DHPR. Therefore, our findings suggest that there must be some underlying tendency of the DHPR to associate with elements of jSR and form dyadic couplings. Furthermore, it seems that since there are apparently no major differences in the molecular composition of the dyads in comparison to skeletal muscle triads, that differences in the primary amino acid sequences of the cardiac isoforms of the RyR (1, 40, 42) and the DHPR (38) may be responsible for the observed differences in the mechanisms of skeletal and cardiac muscle excitation–contraction coupling.

While all the DHPR were localized to the dyadic regions, a substantial proportion of the triadin- and RyR-specific staining was observed to form regularly spaced transverse bands in the interior of atrial cells in the absence of an association with the DHPR. This is consistent with our own and previous ultrastructural observations that many of the feet (RyR) are present in corbular SR or extended junctional SR. However, both the abundance and the regular disposition of the corbular SR at or near the Z-lines, was somewhat unexpected. Although, this latter finding is consistent with the observation that in developing skeletal muscle cells, organization of the SR occurs by an association with cytoskeletal elements prior to its association with the T-tubules (18). In any case, the existence of such an abundance of extended jSR in atrial cells suggests that it will be necessary to determine why some RyR are associated with DHP receptors and others are not, what the role of these "uncoupled" RyR may be, and how they are activated in the absence of a close association with the DHPR.

References

1. Anderson, K., F. A. Lai, Q. Y. Liu, E. Rousseau, H. P. Erickson, and G. Meissner. 1989. Structural and functional characterization of the purified cardiac ryanodine receptor-Ca^{2+} release channel complex. *J. Biol. Chem.* 264:1329-1335.
2. Ashraf, M., W. H. Park, I. Grupp, and A. Schwartz. 1986. Distribution of ^{3}H-nitrendipine in the isolated perfused rat heart as revealed by electron microscopic autoradiography. *J. Mol. Cell Cardiol.* 18:265-272.
3. Ball, Jr., W. J., A. Schwartz, and J. Lessard. 1982. Isolation and characterization of monoclonal antibodies to Na⁺,K⁺-ATPase. *Biochim. Biophys. Acta.* 719:413-423.
4. Block, B. A., T. Imagawa, K. P. Campbell, and C. Franzini-Armstrong. 1988. Structural evidence for direct interaction between the molecular components of the transverse tubule/sarcoplasmic reticulum junction in skeletal muscle. *J. Cell Biol.* 107:2587-2600.
5. Bossen, E. H., J. R. Sommer, and R. A. Waugh. 1978. Comparative stereology of the mouse and finch left ventricle. *Tissue Cell.* 10:773-784.
6. Bossen, E. H., J. R. Sommer, and R. A. Waugh. 1981. Comparative stereology of mouse atria. *Tissue Cell.* 13:71-77.
7. Brandt, N. 1985. Identification of two populations of cardiac microsomes with nitrendipine receptors: Correlation of the distribution of dihydropyridine receptors with organelle specific markers. *Arch. Biochem. Biophys.* 242:306-319.
8. Brandt, N., and A. Bassett. 1986. Separation of dihydropyridine binding sites from cardiac junctional sarcoplasmic reticulum. *Arch. Biochem. Biophys.* 244:872-875.
9. Brandt, N. R., A. H. Caswell, J. P. Brunschwig, J. J. Kang, B. Antoniu, and N. Ikemoto. 1992. Effects of anti-triadin antibody on Ca^{2+} release from sarcoplasmic reticulum. *FEBS (Fed. Eur. Biochem. Soc.) Lett.* 299:57-59.
10. Brandt, N. R., A. H. Caswell, S. A. Lewis Carl, D. G. Ferguson, T. Brandt, J.-P. Brunschwig, and A. Basset. 1993. Detection and localization of triadin in rat ventricular muscle. *J. Membr. Biol.* 131:219-228.
11. Caswell, A. H., N. R. Brandt, J. P. Brunschwig, and S. Purkerson. 1991. Localization and partial characterization of the oligomeric disulfide-linked molecular weight 95,000 protein (triadin) which binds the ryanodine and dihydropyridine receptors in skeletal muscle triadic vesicles. *Biochemistry.* 30:7507-7513.
12. Cleemann, L., and M. Morad. 1991. Role of Ca^{2+} channel in cardiac excitation-contraction coupling in the rat: evidence from Ca^{2+} transients and contraction. *J. Physiol. Lond.* 432:283-312.
13. Curtis, B. M., and W. A. Catterall. 1986. Reconstitution of the voltage-sensitive calcium channel purified from skeletal muscle transverse tubules. *Biochemistry.* 25:3077-3083.
14. Dolber, P. C., and J. R. Sommer. 1984. Corbular sarcoplasmic reticulum of rabbit cardiac muscle. *J. Ultrastruct. Res.* 87:190-196.
15. Ellis, S. B., M. E. Williams, N. R. Ways, R. Brenner, A. H. Sharp, A. T. Leung, K. P. Campbell, E. McKenna, W. J. Koch, A. Hui, A. Schwartz, and M. M. Harpold. 1988. Sequence and expression of mRNAs encoding the α1 and α2 subunits of a DHP-sensitive calcium channel. *Science (Wash. DC)* 241:1661-1664.
16. Fabiato, A. 1983. Calcium-induced release of calcium from the cardiac sarcoplasmic reticulum. *Am. J. Physiol.* 245:C1-14.
17. Fabiato, A. 1989. Appraisal of the physiological relevance of two hypothesis for the mechanism of calcium release from the mammalian cardiac sarcoplasmic reticulum: calcium-induced release versus charge-coupled release. *Mol. Cell Biochem.* 89:135-140.
18. Flucher, B. E., H. Takekura, and C. Franzini-Armstrong. 1993. Development of the excitation contraction apparatus in skeletal muscle: association of sarcoplasmic reticulum and transverse tubules with myofibrils. *Dev. Biol.* 160:135-147.
19. Flucher, B. E., S. B. Andrews, S. Fleischer, A. R. Marks, A. Caswell, and J. A. Powell. 1993. Triad formation: organization and function of the sarcoplasmic reticulum calcium release channel and triadin in normal and dysgenic muscle in vitro. *J. Cell Biol.* 123:1161-1174.
20. Forbes, M. S., L. A. Hawkey, and N. Sperelakis. 1984. The transverse-axial tubular system (TATS) of mouse myocardium: its morphology in the developing and adult animal. *Am. J. Anat.* 170:143-162.

21. Forbes, M. S., and N. Sperelakis. 1977. Myocardial couplings: their structural variations in the mouse. *J. Ultrastruct. Res.* 58:50–65.

22. Fozzard, H. A. 1991. Excitation-contraction coupling in the heart. *Adv. Exp. Med. Biol.* 308:135–142.

23. Franzini-Armstrong, C. 1975. Membrane particles and transmission at the triad. *Fed. Proc.* 34:1382–1394.

24. Franzini-Armstrong, C., M. Pincon Raymond, and F. Rieger. 1991. Muscle fibers from dysgenic mouse in vivo lack a surface component of peripheral couplings. *Dev. Biol.* 146:364–376.

25. Inui, M., A. Saito, and S. Fleischer. 1987. Isolation of the ryanodine receptor from cardiac sarcoplasmic reticulum and identity with the feet structures. *J. Biol. Chem.* 262:15637–15642.

26. Iwata, U., H. Hanada, M. Takahashi, and M. Shigekawa. 1994. Ca^{2+}-ATPase distributes differently in cardiac sarcolemma than dihydropyridine receptor a1 subunit and Na^+/Ca^{2+} exchanger. *FEBS (Fed. Eur. Biochem. Soc.) Lett.* 355:65–68.

27. Jewett, P. H., S. D. Leonard, and J. R. Sommer. 1973. Chicken cardiac muscle: its elusive extended junctional sarcoplasmic reticulum and sarcoplasmic reticulum fenestrations. *J. Cell Biol.* 56:595–600.

28. Jewett, P. H., J. R. Sommer, and E. A. Johnson. 1971. Cardiac muscle. Its ultrastructure in the finch and hummingbird with special reference to the sarcoplasmic reticulum. *J. Cell Biol.* 49:50–65.

29. Jorgensen, A. O., and K. P. Campbell. 1984. Evidence for the presence of calsequestrin in two structurally different regions of myocardial sarcoplasmic reticulum. *J. Cell Biol.* 98:1597–1602.

30. Jorgensen, A. O., A. C. Shen, and K. P. Campbell. 1985. Ultrastructural localization of calsequestrin in adult rat atrial and ventricular muscle cells. *J. Cell Biol.* 101:257–268.

31. Jorgensen, A. O., A. C.-Y. Shen, W. Arnold, P. S. McPherson, and K. P. Campbell. 1993. The Ca^{2+}-release channel/ryanodine receptor is localized in junctional and corbular sarcoplasmic reticulum in cardiac muscle. *J. Cell Biol.* 120:969–980.

32. Junker, J., J. R. Sommer, M. Sar, and G. Meissner. 1994. Extended junctional sarcoplasmic reticulum of avian cardiac muscle contains functional ryanodine receptors. *J. Biol. Chem.* 269:1627–1634.

33. Knudson, C. M., K. K. Stang, A. O. Jorgensen, and K. P. Campbell. 1993. Biochemical characterization and ultrastructural localization of a major junctional sarcoplasmic reticulum glycoprotein (triadin). *J. Biol. Chem.* 268:12637–12645.

34. Knudson, C. M., K. K. Stang, C. R. Moomaw, C. A. Slaughter, and K. P. Campbell. 1993. Primary structure and topological analysis of a skeletal muscle-specific junctional sarcoplasmic reticulum glycoprotein (triadin). *J. Biol. Chem.* 268:12646–12654.

35. Lai, F. A., H. P. Erickson, E. Rousseau, Q. Y. Lui, and G. Meissner. 1988. Purification and reconstitution of the calcium release channel from skeletal muscle. *Nature (Lond.).* 331:315–319.

36. Leung, A., T. Imagawa, B. Block, C. Franzini-Armstrong, and K. P. Campbell. 1988. Biochemical and ultrastructural characterization of the 1,4-dihydropyridine receptor from rabbit skeletal muscle. *J. Biol. Chem.* 263:994–1001.

37. Lewis Carl, S. A., I. Gillette-Ferguson, and D. G. Ferguson. 1993. An indirect immunofluorescence procedure for staining the same cryosection with two mouse monoclonal primary antibodies. *J. Histochem. Cytochem.* 41:1273–1278.

38. Mikami, A., K. Imoto, T. Tanabe, T. Niidome, Y. Mori, H. Takeshima, S. Narumiya, and S. Numa. 1989. Primary structure and functional expression of the cardiac dihydropyridine-sensitive calcium channel. *Nature (Lond.).* 340:230–233.

39. Nabauer, M., G. Callewaert, L. Cleemann, and M. Morad. 1989. Regulation of calcium release is gated by calcium current, not gating charge, in cardiac myocytes. *Science (Wash. DC)* 254:800–803.

40. Nakai, J., T. Imagawa, Y. Hakamata, M. Shigekawa, H. Takeshima, and S. Numa. 1990. Primary structure and functional expression from cDNA of the cardiac ryanodine receptor/calcium release channel. *FEBS (Fed. Eur. Biochem. Soc.) Lett.* 271:169–177.

41. Norman, R. I., A. J. Burgess, E. Allen, and T. M. Harrison. 1987. Monoclonal antibodies against the 1,4-dihydropyridine receptor associated with voltage sensitive Ca^{2+} channels detect similar polypeptides from a variety of tissues and species. *FEBS (Fed. Eur. Biochem. Soc.) Lett.* 212:137–142.

42. Otsu, K., H. F. Willard, V. K. Khanna, F. Zorzato, N. M. Green, and D. H. MacLennan. 1990. Molecular cloning of cDNA encoding the Ca^{2+} release channel (ryanodine receptor) of rabbit cardiac muscle sarcoplasmic reticulum. *J. Biol. Chem.* 265:13472–13483.

43. Peng, M., H. Fan, T. L. Kirley, A. H. Caswell, and A. Schwartz. 1994. Structural diversity of triadin in skeletal muscle and evidence of its existence in heart. *FEBS (Fed. Eur. Biochem. Soc.) Lett.* 348:17–20.

44. Rardon, D. P., D. C. Cefali, R. D. Mitchell, S. M. Seiler, and L. R. Jones. 1989. High molecular weight proteins purified from cardiac junctional sarcoplasmic reticulum vesicles are ryanodine-sensitive calcium channels. *Circ. Res.* 64:779–789.

45. Rios, E., and G. Brum. 1987. Involvement of dihydropyridine receptors in excitation contraction coupling in skeletal muscle. *Nature (Lond.).* 325:717–720.

46. Rios, E., J. J. Ma, and A. Gonzalez. 1991. The mechanical hypothesis of excitation-contraction (EC) coupling in skeletal muscle. *J. Muscle Res. Cell Motil.* 12:127–135.

47. Seok, J.-H., L. Xu, N. R. Kramarcy, R. Sealock, and G. Meissner. 1992. The 30S lobster Ca^{2+} release channel (ryanodine receptor) has functional properties distinct from the mammalian channel proteins. *J. Biol. Chem.* 267:15893–15901.

48. Sham, J. S. K., L. Cleemann, and M. Morad. 1993. Functional coupling between the dihydropyridine receptors and the ryanodine receptors of cardiac myocytes. *Biophys. J.* 63:A121.

49. Sommer, J. R. 1982. Ultrastructural considerations concerning cardiac muscle. *J. Mol. Cell Cardiol.* 14(Suppl.)3:77–83.

50. Sommer, J. R., and E. A. Johnson. 1970. Comparative ultrastructure of cardiac cell membrane specializations. A review. *Am. J. Cardiol.* 25:184–194.

51. Sommer, J. R., and R. A. Waugh. 1976. The ultrastructure of the mammalian cardiac muscle cell—with special emphasis on the tubular membrane systems. A review. *Am. J. Pathol.* 82:192–232.

52. Stern, M. D., and E. G. Lakata. 1992. Excitation-contraction coupling in the heart: state of the question. *FASEB (Fed. Am. Soc. Exp. Biol.) J.* 6:3092–3100.

53. Sun, X.-H., F. Protasi, M. Takahashi, H. Takeshima, D. G. Ferguson, and C. Franzini-Armstrong. 1995. Molecular architecture of membranes involved in excitation contraction coupling of cardiac muscle. *J. Cell. Biol.* 129:659–671.

54. Takahashi, M., and W. A. Catterall. 1987. Dihydropyridine sensitive calcium channels in cardiac and skeletal muscle membranes: studies with antibodies against the alpha subunits. *Biochemistry.* 26:5518–5546.

55. Takeshima, H., S. Nishimura, T. Matsumoto, H. Ishida, K. Kangawa, N. Minamino, H. Matsuo, M. Ueda, M. Hanaoka, T. Hirose, and S. Numa. 1989. Primary structure and expression from complementary DNA of skeletal muscle ryanodine receptor. *Nature (Lond.).* 339:439–445.

56. Tanabe, T., K. G. Beam, B. A. Adams, T. Niidome, and S. Numa. 1990. Regions of the skeletal muscle dihydropyridine receptor critical for excitation-contraction coupling. *Nature (Lond.).* 346:567–569.

57. Tanabe, T., K. G. Beam, J. A. Powell, and S. Numa. 1988. Restoration of excitation contraction coupling and slow calcium currents in dysgenic mice by dihydropyridine receptor complimentary DNA. *Nature (Lond.).* 336:134–139.

58. Tanabe, T., H. Takeshima, A. Mikami, J. Flockerzi, H. Takeshia, K. Kangawa, M. Matsuo, T. Hirose, and S. Numa. 1987. Primary structure of the receptor for calcium channel blockers from skeletal muscle. *Nature (Lond.).* 328:313–318.

59. Tokumaru, H., K. Anzai, T. Abe, and Y. Kirino. 1992. Purification of the cardiac 1,4-dihydropyridine receptor using immunoaffinity chromatography with a monoclonal antibody against the alpha 2 delta subunit of the skeletal muscle dihydropyridine receptor. *Eur. J. Pharmacol.* 227:363–370.

60. Vaghy, P. L., J. Streissneg, K. Miwa, H.-G. Knaus, K. Itagaki, E. McKenna, H. Glossman, and A. Schwartz. 1987. Identification of a novel 1,4-dihydropyridine- and phenylalkylamine-binding polypeptide in calcium channel preparations. *J. Biol. Chem.* 262:14337–14342.

61. Zorzato, F., J. Fujii, K. Otsu, M. Phillips, N. M. Green, F. A. Lai, G. Meissner, and D. H. MacLennan. 1990. Molecular cloning of cDNA encoding human and rabbit forms of the Ca^{2+} release channel (ryanodine receptor) of skeletal muscle sarcoplasmic reticulum. *J. Biol. Chem.* 265:2244–2256.